ANALYSIS OF FACTORS AFFECTING PEAK TO AVERAGE RATIO AND MEAN POWER IN WAVE ENERGY CONVERTER MODELS USING REGULAR AND IRREGULAR WAVES

A thesis presented to the faculty of the Graduate School of
Western Carolina University in partial fulfillment of the
requirements for the degree of Master of Science in Technology

By
Connor McIntyre

Director: Dr. Bora Karayaka
Associate Professor
School of Engineering and Technology

Committee Members:
Dr. Adams - Electrical Engineering, School of Engineering and Technology
Dr. Kaul - Mechanical Engineering, School of Engineering and Technology
Western Carolina University
Cullowhee, USA

March 2020

ACKNOWLEDGEMENTS

I would like to acknowledge the efforts and resources of Western Carolina University for giving me the ability to complete this thesis. WCU has been a place of learning and discovery for the 6 years for me as my undergraduate was here as well. Specifically, I want to thank my advisors and committee members for giving guidance over the duration of this thesis project. Whom without I would not be where I am today. To a slightly lesser extent I would like to thank every professor or teacher who has taught me, their foundations of education ingrained in me allowed me to reach new heights of knowledge. Thank you.

TABLE OF CONTENTS

LIST OF TABLES

LIST OF FIGURES

ABSTRACT

Analysis of Factors Affecting Peak to Average Ratio and Mean Power in a Slider Crank Wave Energy Converter using regular and irregular waves

Connor McIntyre

Western Carolina University (April 2020)

Director: Dr. Bora Karayaka

This thesis investigates the factors that affect the Peak to Average Ratio (PTAR) and Mean Power (MP) for the Slider Crank Wave Energy Converter (SCWEC). The goal of this thesis is to reduce the PTAR while maximizing the MP. The PTAR needs to be reduced, because the generator that converts wave energy to electricity for the grid would become more efficient and less costly. During the process of minimizing the PTAR, the impact on MP production should be minimized, since producing usable power is the main purpose of any generation mechanism. In this thesis, a few system parameters affecting the PTAR and the MP are investigated and analyzed. In this analysis, these parameters are applied to multiple models of the system, and the results are recorded and compared. It is observed that the best combination of the PTAR and the MP can be determined under regular wave conditions as well as irregular wave conditions. Some of the factors that affect PTAR and MP include phase and time delay. Inertia additionally had an effect on both but was minimal.

CHAPTER 1: INTRODUCTION

1.1 Key Terms

Mean Power (MP): Average Power produced by the WEC in the given time period

Peak to Average Ratio (PTAR): Ratio between the highest value of power produced and average power produced during steady state.

Power Take Off System (PTOS): This refers to the mechanical front end of the WEC, the buoy and slider crank.

Wave Energy Converter (WEC): A wave energy converter is a device that converts the kinetic and potential energy associated with a moving wave into useful mechanical or electrical energy.

1.2 Problem Statement

Energy usage and consumption around the world is currently at an all-time high. It is also expected to increase into the future. This is due to many factors including new technologies, higher population and greater access to said technologies. In 2013 humans used 5.67×10^{20} joules of energy, equivalent to about 18.0 terawatt-hour (TWh)[1]. A majority of those joules that were used were produced via fossil fuels. It is agreed upon by many that the worlds' fossil fuels are being diminished at a rate that far exceeds the production of them. In short, we are running out of fossil fuels. The most common form of energy that is used worldwide is electrical energy. There are thankfully solutions to this growing problem.

Renewable energy is a practical way to produce more energy for humans to use. There are many ways that power can be produced from natural phenomena. The general process is to take a force that occurs naturally then turn that force into rotational motion to turn a generator. Another way is to use solar energy to gather the sun's rays and send that energy to the grid. A problem that occurs with both ways is that the power produced is very inconsistent. You might have a lot of

sunlight and wind one day and none on the next. That is just one of the challenges that must be overcome to better harvest energy from renewable sources. A slightly more consistent method of renewably sourcing energy is with ocean wave power. This is because while waves do change over time, they, are generally not bound to follow a day and night cycle like wind and solar are.

Waves occur naturally in our oceans and lakes and can form from the tides, currents, or even wind. Depending upon the weather conditions around the Wave Energy Converter (WEC) power produced can be quite consistent. "Presently, about 40% of the world's population lives within 100 kilometers of the coast" [2]. Power is best produced where it is used because it saves on transmission loses. WECs are found near coastlines because water is pushed up by the landmass and more energy can be extracted. A common design for WECs is to have a buoy floating on top of the water and when a wave passes by the buoy is displaced and rotates a shaft in a generator. This method has been proven to work and is currently in use. This type of design is not without its problems.

When the buoy is pushed up from its own buoyancy it causes a high torque on the generator shaft. This is good because higher torque means more energy output. The hydrodynamic forces acting on a wave energy capture device is geometry specific. For example, the forces when the buoy is pushed may not be the same when the buoy is sinking, which results in irregularity of forces that need to be dealt with in a specific WEC design. The generator, inverter and all the other components must be rated for the highest amount of power produced. Because of these components the costs of implementing a WEC system is increased even though it only produces that peak power for a short time every cycle.

This thesis aims to answer the following questions, First; To what extent can PTAR be reduced without sacrificing Mean Power? Second; Is modification of inertia beneficial to the WEC

by Reducing PTAR and maintaining MP? Third; What parameters affect the PTAR and MP? All of these questions must be investigated with both regular and irregular waves as to provide accurate real-world data.

The outline of this thesis is organized as follows: Chapter 2 describes the literature review, research on related papers and topics for reducing the PTAR. Chapter 3 describes the methods that are used to develop the models of the systems as well as the models themselves. Chapter 4 shows the results of the models used in this analysis. Finally, conclusions and future works are described in Chapter 5.

CHAPTER 2: LITERATURE REVIEW

This chapter describes some ways that Wave Energy Collectors ,WEC, extract their energy. This information was gathered from multiples sources in a literature review. It also describes some of the issues with WECs and some potential solutions to the issues such as flywheels.

2.1 **Wave Energy Extraction Techniques**

Wave energy is a renewable energy source that has seen some rise in popularity in the last decade. The basic idea is to take energy from waves through the motion of the water. This energy is later transferred to a generator and is send to the grid for common use. There are many different designs for wave energy generators, some simply move up and down capturing the vertical motion of the wave with a buoy, some hold water in a tank and release it through a turbine. There are even hybrid systems that use multiple forms of renewable energy together to provide more consistent power to the grid [3]. Waves acquire their motion through wind, ocean currents and even the shape of the ground beneath them. Because waves add to other waves, each one is a unique summation of its components. This means that outside of a lab simulation no wave generator will be able to perfectly match the waves it simulated nor the energy extracted. To extract a general amount, different designs use different components of the wave's total energy. For example, a slider crank system focuses on the vertical motion, the heave component of the wave set, to turn a shaft and generate power.

2.2 **Problems with Wave Energy**

However, wave energy generation like most other renewable energy is very inconsistent. It relies upon forces of nature which are inherently unpredictable. "Wind turbine provides highly variable power to the grid. To smooth this power, the storage device exchanges power with an external network in order to smooth the power flow." [4]. When power is produced through these devices there are many peaks and valleys in the power curve. This is not optimal for putting said power back onto the grid. Ideally power

sent to the grid should be a constant value, something easily achievable for a nuclear reactor and gas fed turbines but not so for a wave energy generator. Some designs of wave energy generators take this into account, somehow storing the energy. For example, there is a design that uses the height of the water in a tank as a way to regulate the energy output. The tanks' intake of water is dependent upon the waves, but it constantly releases water through a turbine, so the power out is more consistent. [5]

One of the most common problems with wave energy generators is the peak to average power ratio [6]. Having a high ratio makes the PTOS components have to be rated for the highest peak amount produced. The system used was modeled with common sinusoidal waves of the same height. While this is not exactly what goes on in nature it is close enough to experiment with another variable, positioning. The next simulation that was performed was using linear sets of seven life ring WECs organized in a way to funnel the waves to the last set of seven. When the system was in sync with itself it reduced the peak to average ratio. Having the WECs in the type of configuration was found to reduce the peak to average from ten down to three. They went on to further discuss the reduction down to two when they added more friction to the system. This made the system overall less efficient but had a better ratio. [6]

Another way to regulate output power to be more consistent is to store the power in some way. This can be with batteries, capacitors or through physical means. One of the ways to store power is to use a Flywheel Energy Storage System (FESS). A FESS uses the rotating kinetic energy to store the energy. It can be reused multiple times and has been shown to work with similar renewable energy systems. In one journal article, [3] a flywheel is used to manage a wind turbine and is proven to smooth the power output. A wind turbine is very similar electrically to a wave energy generator. They both have varying natural conditions which lead to large fluctuations in the power output. In the journal article the feedback loop that they use to control the angular speed is shown. Additionally, the authors explain that they keep the flywheel within a certain range of angular speed, by varying the torque applied. The wind power system was simulated using MATLAB Simulink to find the results of the feedback loop.

It is very important to model the flywheel correctly accounting for losses, efficiency and state of charge. There were several equations that help model it in this article [7]. The researchers in this article

also used a wind farm but with a wave energy system regulated through a flywheel energy storage system. They placed the FESS after the wind and wave power and before it is sent to the grid. Having this configuration means that if they ever max out the capacity of the flywheel, then the power that is sent to the grid is back to being noisy. When the FESS is in a steady state it should adjust the amount of output power to meet the average rate coming from its source(s). In this paper an 80 MW wind turbine, a 40-MW wave energy collector were used in conjunction, and they were able to derive the stability of the simulated system. They concluded that the FESS was effective at raising the bus voltage and smoothing the active power fluctuations. They also derived the "complete dynamic equations of the studied system under three-phase balanced loading conditions" [7]

When designing/modeling the wave energy converter model, one should keep in mind the limitation of using regular waves. Along with that WEC simulation the flywheel energy storage system must have proper parameters to smooth the input power. A FESS works best within limited range but still achieving the stability. Using a FESS has already been proven to work with wind power smoothing. Below in Fig. 2.1 shows the physical model of the slider crank WEC.

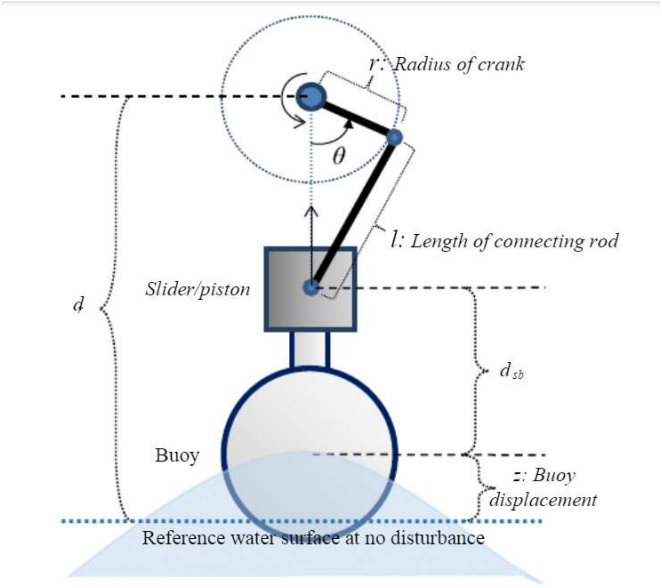

Fig 2.1 Example of a Slider Crank WEC Side View

CHAPTER 3: METHODOLOGY and MODELS

This chapter describes the system models used to simulate the slider crank WEC. To quote the statistician George Box "All models are wrong but, some are useful". The models are only so accurate and verification with real world models still needs to be investigated. This section provides insight on how these models are formed and how they function.

3.1 Overall System Models

The model(s) of this system are designed in MATLAB™/Simulink™ environment. In this study, a couple of models were employed, the first at a relatively basic level and then with adding complexity. The results of the models can be compared to one another since the details of the basic model are inherent to the more complex one.

In the first model (Fig 3.1), the topology is more focused on the back-end in comparison to the complete SC-WEC model in Fig. 3.2. Both models are initialized with a separate MATLAB script that determines the wave height and frequency. In these cases, the waves were all of the same height (1 meter) and with varying wave periods. Simulink is a block-based Graphical User Interface for MATLAB and, in theory everything that is shown in (Fig 3.1) and (Fig 3.2) can be recreated in a script. This was achieved for the model in Fig. 3.2, making it quite easy to modify the system variables so that the impact on the PTAR and MP analysis can be streamlined. Most of the graphs and figures in this study relied on 2D and 3D plotting functionality of the programming environment.

3.2 Simplistic Rotational WEC Back End

The model in Fig. 3.1 represents the first order equation of motion for a rotational WEC system back-end.

$$J\frac{d\omega}{dt} + B\omega = T_{PTO} - T_{EL} \qquad (1)$$

$$P_{EL} = T_{EL}\omega \qquad (2)$$

where J is system inertia constant in kg.m^2, B is viscous damping constant in Nm.s/rad, T_{PTO} and T_{EL} are WEC-PTO and electromechanical torque respectively, P_{EL} is the electromechanical power produced and ω is the angular velocity in rad/s.

In the second model shown in Fig. 3.2, the motion of the buoy is assumed to be riding centered at a tangent point of the wave and is assumed to be half submerged. The equation that resolves the forces of the wave into the forces on the crank shaft of the generator is shown in (3).

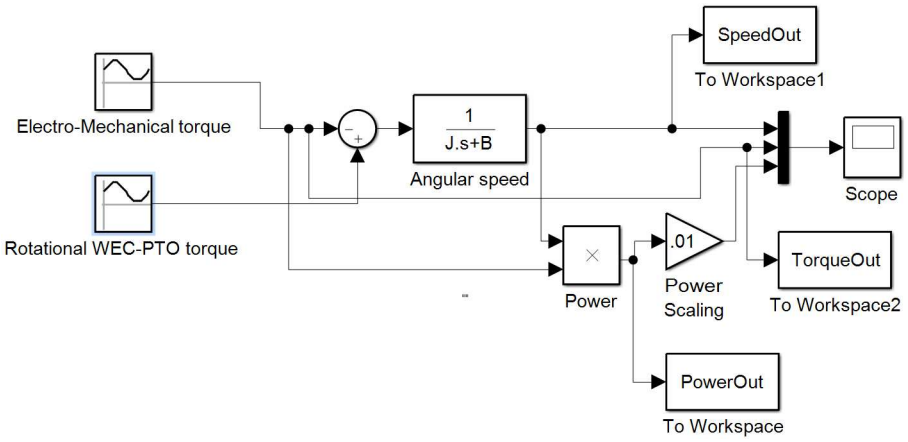

Fig. 3.1 Model of a simple rotational WEC system back-end

$$(M + a_\infty)\ddot{z}(t) + \int_{-\infty}^{t} H_{rad}(t-\tau)\,\dot{z}(\tau)d\tau + S_b z(t)$$

$$= F_e(t) - F_u(t) \quad (3)$$

where M is the physical mass of the buoy, a_∞ is the buoy-added mass at an infinite wave period, z is the buoy center of the gravity displacement in the heave direction, H_{rad} is the radiation impulse response function. Furthermore, S_b is the hydrostatic stiffness, F_e is the wave excitation force, and F_u is the PTOS' reactionary force [8]. The reactionary forces are primarily caused by the generator functioning although there are other sources including friction and inertia. These reactionary forces take energy away from the PTOS. In the case of the generator it is purposeful, generating electricity, however with other reactionary forces the end outcome is losses.

3.3 Complex Rotational WEC with Resonance Control Strategy

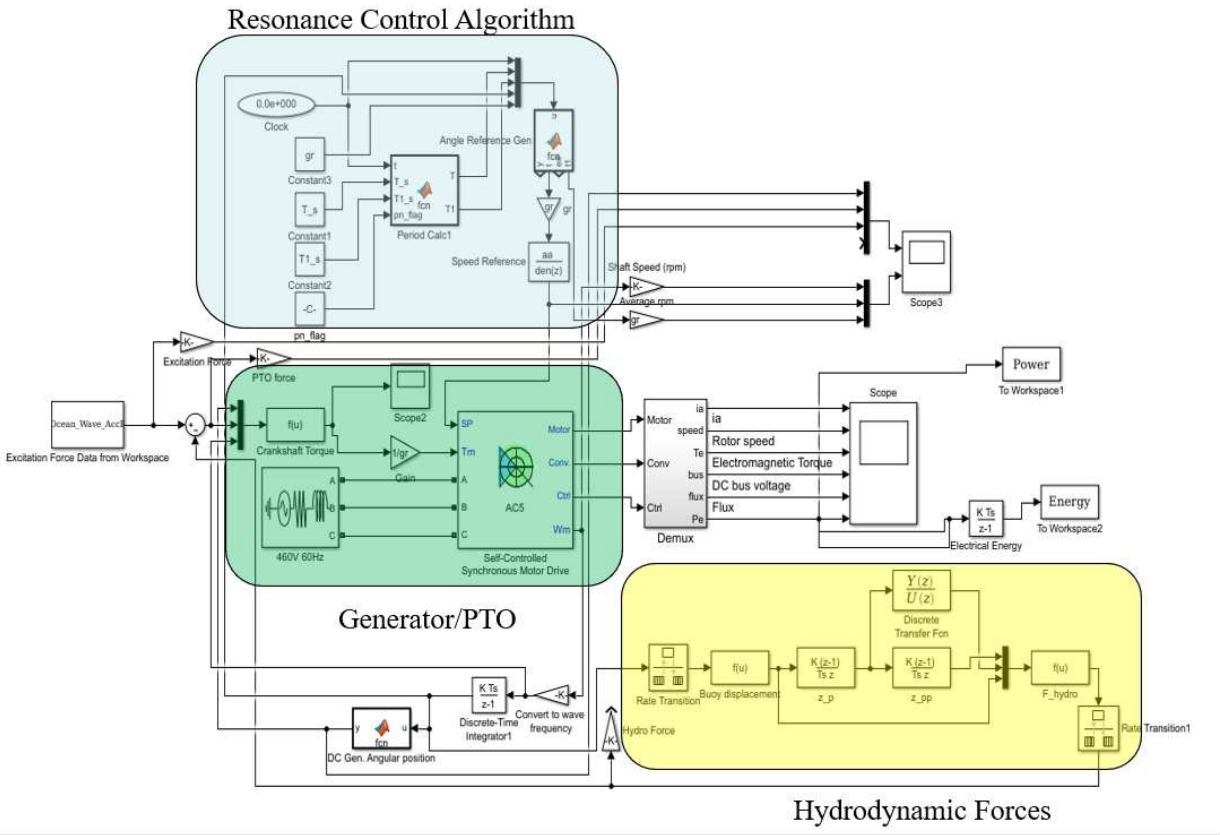

Fig. 3.2 Model of SC-WEC with wave resonance control system

The blocks in the bottom right corner of Fig. 3.2 realizes the right side of (3). The wave excitation force F_e (the left most block) in Fig. 3 is preprocessed based on the specific wave pattern (characterized by period, height, regularity/irregularity) for semi-submerged spherical buoy geometry. F_e is used in the calculation of F_u which moves slider up and down in Fig. 2.1. Corresponding rotational torque produced by slider crank linkage is evaluated by "Crankshaft Torque" block in the left middle part of Fig. 3.2. This torque eventually rotates the synchronous machine (largest block in Fig. 3.2 located towards the middle) for power production. The machine's speed is controlled by the resonance or phase-lock control algorithm, which is realized by the blocks in the upper left corner of Fig. 3.2.

This resonance control algorithm was effectively used by the WEC to control the motion of the buoy. This in turn helps regulate the power output of the generator. It achieves this by varying the electromagnetic torque of the generator itself. For example, imagine the waves powering the PTOS having a longer or shorter period then average. The control strategy will change the electromagnetic torque of the generator which will reduce or increase the reactionary force of the crankshaft. This then allows it, the WEC, to sync up with the PTOS which is directly based off the waves motion again.

While the process itself is a simple idea, the resonance control strategy takes into account many of forces affecting the buoy. With any object there are 6 ways it can move axially, X, Y, Z, also known as surge, sway and heave, and rotatory, yaw, pitch and roll. Thankfully with this Slider-crank WEC (SCWEC) some of these movements aren't possible, such as X and Y, because of the geometry of the SCWEC and the location of the buoy. Fig 2.1 shows the motion and the general geometry of a SCWEC. One of the prominent forces is the buoyancy force caused by the displacement of water by the buoy. This doesn't mean that the other forces are not accounted for in the control algorithm. Some of the other forces include the radiation force, how much the wave is reflected off the buoy, the force required to accelerate the mass of the buoy and of course friction. These forces are applied by the Resonance control strategy to better regulate the motion of the slider crank to be in sync with the wave forces it receives.

The randomness of the waves simulated is regulated by equation (4) and (5). It generally follows approximately a normal distribution and then uses that normal distribution to determine a peak enhancement value. α_j is a nondimensional variable that is a function of the wind speed and fetch length, f_p is the peak frequency of the irregular wave, f is the frequency of the wave components, and γ^{Γ} is the peak enhancement factor. [7]

$$S(f) = \frac{\alpha_j g^2}{(2\pi)^4} f^{-5} \exp\left[-\frac{5}{4}\left(\frac{f_p}{f}\right)^4\right] \gamma^{\Gamma} \tag{4}$$

$$\Gamma = \exp\left[-\left(\frac{\frac{f}{f_p}-1}{\sqrt{2}\sigma}\right)^2\right], \sigma = \begin{cases} 0.07 & f \leq f_p \\ 0.09 & f > f_p \end{cases} \tag{5}$$

$$\alpha_j = \frac{H_{m0}^2}{16\int_0^\infty S^*(f)df} \tag{6}$$

$$S^*(f) = \frac{g^2}{(2\pi)^4} f^{-5} \exp\left[-\frac{5}{4}\left(\frac{f_p}{f}\right)^4\right] \gamma^\Gamma \tag{7}$$

$$H_{m0} = 2\sqrt{2}A \tag{8}$$

In the above equation (6), H_{m0} is the significant wave height of the irregular wave (8), and according to the equal energy transport theorem significant waves heights (7) are determined. Where A is the amplitude of the regular sinusoidal wave with equal energy. So that the irregular wave has the same amount of energy as the regular equivalent.

The model utilizing the resonance control algorithm did have some limits, however. Mainly that it was limited to some specific waves sets with regular waves. This also translated to irregular waves because of how the average wave set was determined. The sets that it was limited to are the 6,7,8,9,10 sec wave periods. There were wave sets that are needed to be included specifically the 5 and 11 sec wave sets. To have these sets in the code new cases were made for each. Then specific integral formulas were solved with Wolfram Alpha™ for the coefficients used in each case. Once these cases were added to the code it allowed for a broader set of waves to be studied.

CHAPTER 4: ANALYSIS and RESULTS

Chapter 4 is the bulk of the research of this thesis. In this section all of the different studies are performed along with some analysis of the data collected. Each study used a different model or different parameters some building from the conclusions of the previous study. Both regular and the more real world-like irregular waves were used in this section.

4.1 A Case Study of Changing Phase Angle and Bias of the Generator with Regular Waves

This study was one of the first analyses investigated for this thesis. It used a basic model (as shown in Fig. 3.1) which served to give insight on how the more complicated models would look and behave with regular waves. There were six different phases and five biases for each of them. In Fig.4.1a/4.1b each of the different phases is represented by a different color, the biases in Nm is measured in the hundreds and the power is measured in watts. The phases were $\pi/6$, $\pi/3$, $\pi/2$, $2\pi/3$, $5\pi/6$, π and the biases were 100,200,300,400,500. Each of these combinations as biases and phases gave a very similar graph seen in Fig 4.4. In that figure yellow is output power, blue angular speed of shaft and red required generator torque. Bias in this study refers to the average torque required by the generator, the middle of the red sine wave in Fig. 4.2.

Some observations to note here are that as the bias increased the power fluctuations decreased. Another observation is that as the bias was increased the mean power increased and then later decreased. This implies that there is a peak point where a specific bias provides the maximum mean power. It should be noted that there wasn't much difference between the different phases. While this wasn't properly investigated this is most likely due to the simplicity of the analysis used. From Fig. 4.2 one can see that once the generator reaches steady state the power produced steadily increased.

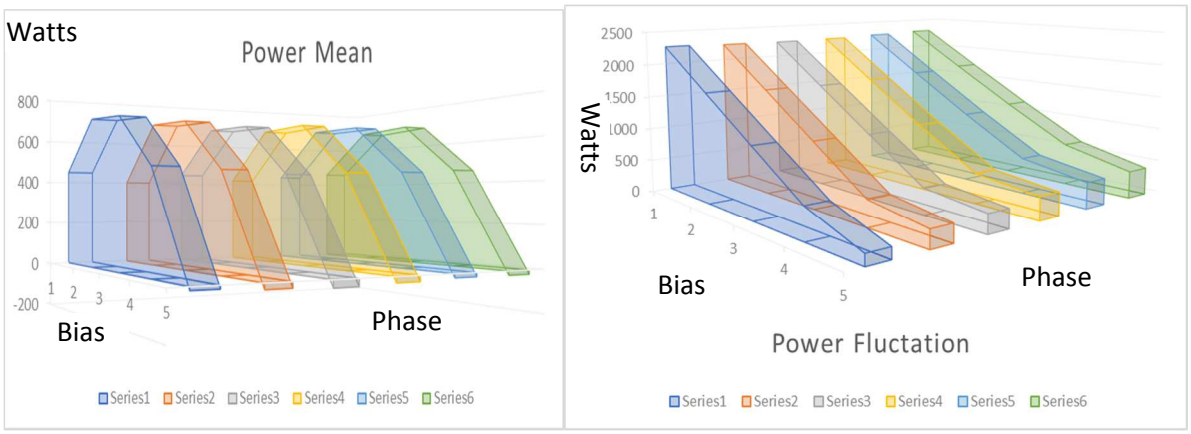

Fig. 4.1a and 4.1b Initial study with phase and generator bias with basic model

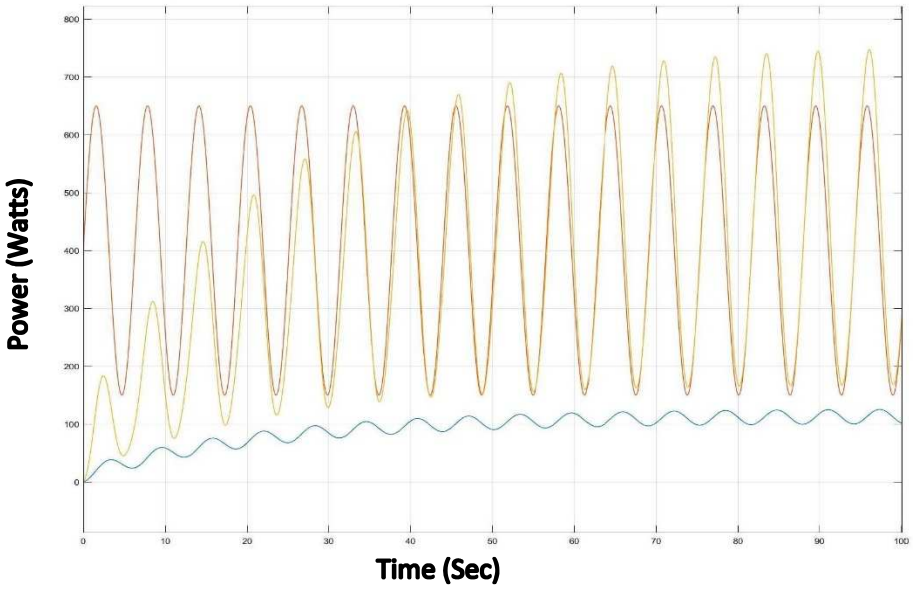

Fig. 4.2 Workspace graph with Output power, Shaft speed, Required torque

4.2 Study of Bias and Phase with Regular Waves in Simple Model

In this study, the more basic model (Fig 3.1) is used along with the program script equivalent for solving the governing differential equation. Since the patterns of wave energy are nearly impossible to control, it is much easier to make adjustments to the generator. As a result, effective means of influencing the output and thus the PTAR/MP is to vary the parameters of the generator and controller. The parameters that were varied in this study were the Bias and the Phase.

"Bias" is how much average T_{EL} is required by the generator to function in a WEC environment. This is called the "fixed torque" in the model. There is also a "fluctuating torque" component in the model, or the variation in T_{EL} required by the generator, but that remained constant for the different biases tested. The range of torque tested for the bias in this study was 25 to 150 *Nm*. This system was simplified down to (Fig4.3) where there is both the fluctuating and the constant part of the torque. Assumed variation of T_{EL} and T_{PTO} are defined by (9) and (10).

$$T_{EL} = T_{EL\_bias} + T_{EL\_fluct} \sin(\omega_{wave} t + \theta) \qquad (9)$$

$$T_{PTO} = T_{PTO\_bias} + T_{PTO\_fluct} \sin(\omega_{wave} t) \qquad (10)$$

where T_{EL_bias} is the bias or average value of T_{EL}, T_{EL_fluct} is the fluctuation amount in T_{EL}, ω_{wave} is the ocean wave's angular frequency, θ is the phase angle for T_{EL} variation in reference to T_{PTO}, T_{PTO_bias} is the bias or average value of T_{PTO} and, T_{PTO_fluct} is the fluctuation amount in T_{PTO}.

"Phase" is a representative of how well the generator torque and the WEC-PTO torque synchronized. The phase range in this study was $0 - 2\pi$ i.e. a full rotation around the unit circle. In Fig. 4.3, the transfer function $\Omega(s)/T(s) = 1/(Js + B)$ and associated variables given in (9) and (10) are represented using the principle of superposition. The results based on the calculations with (Fig. 4.3) were then plotted to see the effect of the variables on the peak to average ratio and the average power. The calculations used 50 equally

spaced bias and phase values. The differential equation solver was run for 50×50 times to calculate corresponding the PTAR and the MP values. During these simulations, the variables that are kept constant are as follows: $B = 0.875\ Nm.s/rad$, $J = 30\ kg/m^2$, $T_{EL\_fluct} = T_{PTO\_fluct} = 250\ Nm$, $T_{PTO\_bias} = 150\ Nm$, $\omega_{wave} = 1\ rad/s$. The results of these simulations are provided in Fig. 4.4.

Additional investigation was conducted with increased inertia values. It was observed that the PTAR values were effectively reduced in larger bias differences while the MP values stayed relatively constant.

From (Fig.4.4) a few observations can be more easily made. First, in the green surface of the MP, the closer the phase is to zero or 2π, the lower the average power is. This result is as expected where the more in sync the electromechanical torque is with the PTO torque, the less power is produced. The bias difference ($T_{PTO\_bias} - T_{EL\_bias}$) had a similar effect on the average amount of power produced. In (Fig.4.4) the green dome shaped surface is the MP and overlaid with the PTAR surface in red. It is important to note in (Fig.4.4) that while the PTAR is unitless and the MP is measured in kilowatts, the MP had to be scaled down so the comparison is more clear. One of the bigger challenges with wave energy generators is the peak to average power ratio [8]. While it is possible to reduce the PTAR even more as the red graph indicates, the average power that is produced decreases dramatically as well. Both the bias and the phase had drastic effects on the PTAR. As phase decreased, the PTAR also increased. The more in phase T_{EL} was with T_{PTO}, the greater the PTAR. It was also observed that as the bias difference is at the extremes, the PTAR reached its extreme values as well. Therefore, these results show that there is a delicate balance between the MP and the PTAR. As the PTAR is reduced, sacrifices in the MP must be made.

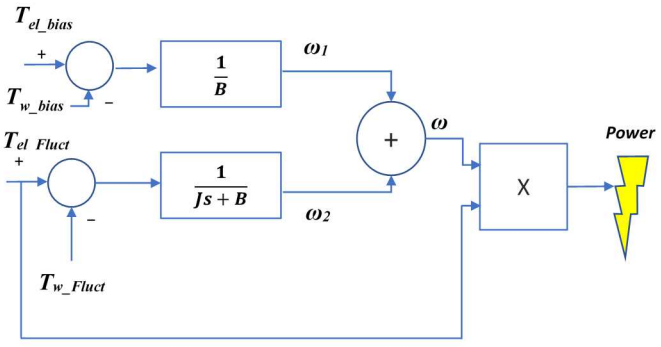

Fig.4.3 Model of rotational WEC with the torque components

In (Fig. 4.3), the symbols ω_1, ω_2 refer to the rotational speed of the shaft with fluctuating and average components. In Fig.4.4, the peak MP occurs at θ=2.17 *rad* and a bias difference of 43.36 *Nm*. The graph has been scaled down by a factor of 500 and the maximum value of MP is 8.18 kW. This peak point has a corresponding PTAR value of 3.91. A few other points on the surface have been investigated around this peak MP point and some comparisons are made. A 2.5% change in the PTAR has an associated 6% reduction in the MP. This trend becomes even more dramatic the farther from the peak MP one gets. As the 3D surfaces clearly reveal, an attempt to reduce the PTAR has to be traded with a larger reduction in the MP.

In this 3D surface plot of the MP and the PTAR, the x-axis represents the bias difference ($T_{PTO\_bias} - T_{EL\_bias}$) and the y-axis represents the phase (θ).

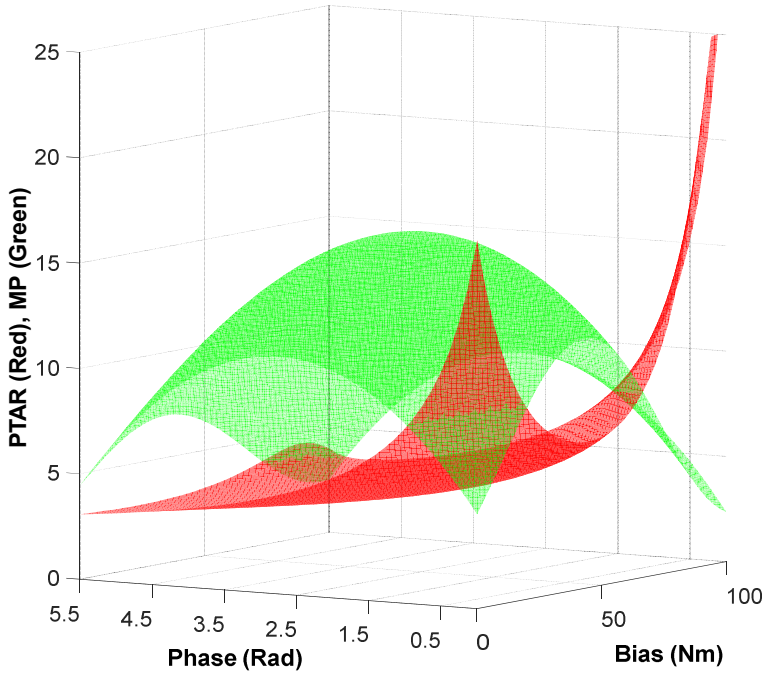

Fig.4.4 3D surfaces of PTAR (red) and MP (green) in an elementary rotational WEC system

4.3 Study of Phase and Time delay in Complex WEC System with Regular Waves

In this step of the investigation, the more complex WEC system (Fig.3.2) has been used. A similar study was conducted in the literature to maximize MP only [10]. In this study, the parameters modified for testing were phase difference and wave frequency. The phase difference identifies the phase difference between wave excitation force $F_e(t)$ and the buoy velocity functions. Normally, these two functions are in-phase for reactive control methodology applied in this WEC system [10]. The reason for not modifying bias with this model is that increased T_{EL} results in increased angular speed. Since a resonance control mechanism was utilized in this WEC model, angular speed needs to be kept at a value proportional to the wave frequency. Therefore, this prevents the user from modifying T_{EL} bias unless the control algorithm is fundamentally modified.

The simulation was run over 500 seconds and data points were collected for each wave frequency set. The wave frequency sets were regular waves with heights of 1 meter and frequencies of 1/5, 1/6, 1/7, 1/8, 1/9, 1/10, 1/11 Hz. The phase difference (or time delay) range was from −1.5 seconds to 1.5 seconds. This means that, in the simulation, the time it took for the wave to travel one cycle or peak to peak was 5, 6...11 seconds. With each of the different wave sets the same range of time delay was used, i.e. −1.5 s to 1.5 s. This made different angle modifiers for each of the wave sets because they had different periods. This angle range was as wide as +/−108 degrees for the 1/5 Hz set and as narrow as +/−50 degrees for the 1/11 Hz set.

Each of the different wave sets was run by modifying the time delay difference by 0.1 seconds for a total of 30 cases for each wave set. The results are shown in Fig. 4.5. At the end of each simulation, MP and PTAR values were first collected and then graphed. Only the data in the angle range of −50 to 50 degrees was used for consistency, since the values outside this range resulted in large deviations in PTAR and MP. Once the PTAR data points for each of the wave sets was

collected and graphed, a polyfit curve (in MS Excel^{TM}) was created for each to determine their lowest PTAR. Then the global minimum PTAR of all of the waves together was calculated by using the polyfit function again. That was determined to be a PTAR of about 2.5 and that occurred at around −14 degrees. This means that the lowest PTAR happens when there is a varying time delay of −0.1 to −0.2 seconds depending on the wave sets of 1/5 Hz to 1/11 Hz. It was also observed that overall PTAR values decreased with decreasing wave frequencies.

There was another brief study done with the data and that compared the MP to the phase difference angle (Fig. 4.6). This study showed that the overall maximum MP was produced when there was an angle of zero (as expected from the linear potential flow theory). It was observed that the maximum power on average was produced when there was no angle difference or no time delay.

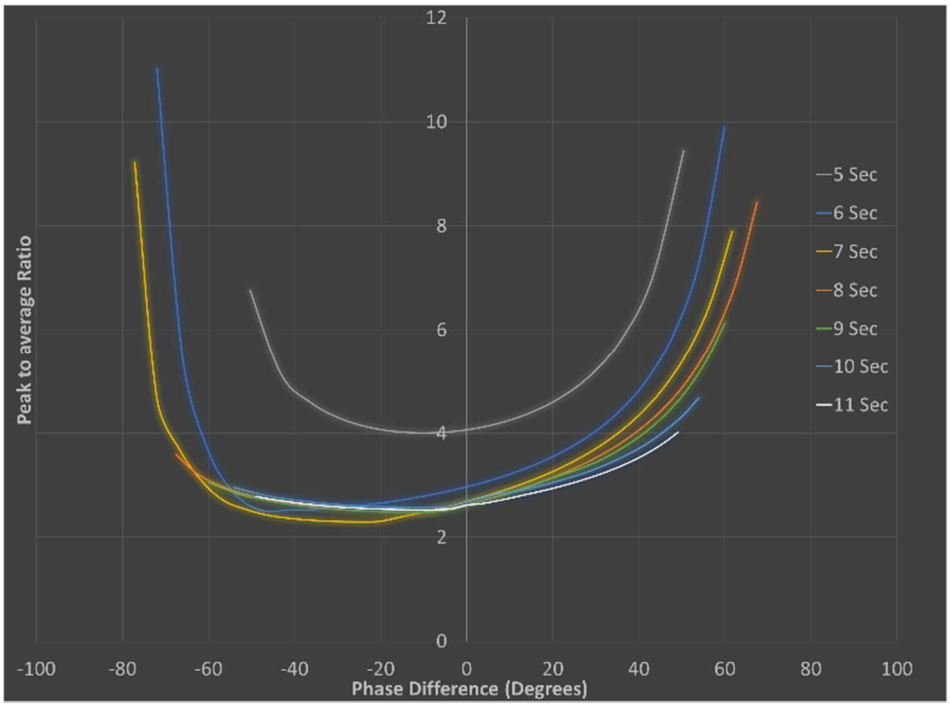

Fig.4.5 The PTAR of wave sets with varying period vs phase difference in degrees

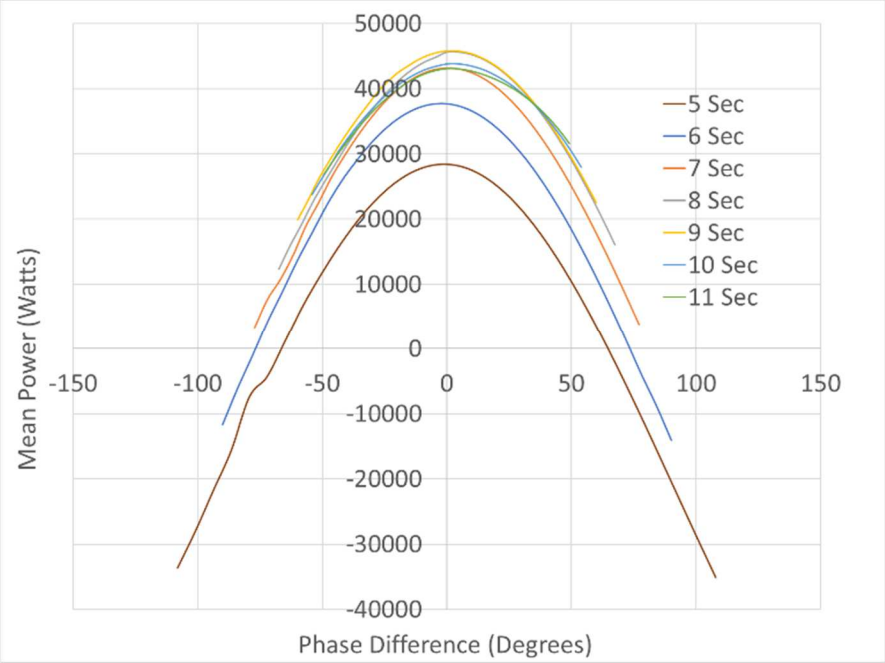

Fig.4.6 Mean power of wave sets with varying periods vs phase difference in degrees

4.4 Best Case Index

These two facts resulted in conflicting outcomes. One that says the lowest/best PTAR needs a time delay of 0.1 s and another that says the greatest/best MP needs a zero time delay. One way to resolve this issue is via a best-case index. This allows for weights to be put on each of the variables and then the sum of each weighted variable is compared to one another. The idea of the best-case index is to minimize the value of PTAR and maximize the value of MP for the purpose of achieving most cost-effective operation corresponding to the largest value of best-case index. To create this best-case index (*BCI*), first the average PTAR and average MP for the entire range of values must be calculated. Then that value(s) is(are) divided by each of the respective PTAR or MP for the specific value that is being observed. For PTAR, the goal is to minimize, so the variable must be in the denominator or raised to the power of −1. For MP, the goal is to maximize, so the variable must be in the numerator. Each of the two variables is then divided by their respective overall

average value to arrive at normalized values. Next the normalized values are multiplied by their weights. Finally, the numbers are summed together to give a numerical value with which that set of data can be evaluated. This is expressed in (11) below. With this equation, the weights assigned to each variable are arbitrary as there is no specific metric or guideline to put more importance on PTAR or MP. However, a case study can be put forth for a specific range of weights. Therefore, using this weighted approach (11), one can maximize *BCI* for a specific range of *W1* and *W2*.

$$BCI = W1 * \left(\frac{PTAR}{PTAR_{Avg}}\right)^{-1} + W2 * \left(\frac{MP}{MP_{Avg}}\right) \qquad (11)$$

Table 4.1 lists the evaluated *BCI* values for different weights and wave periods. With this method the greater the number the better. Highlighted green rows show the largest overall *BCI* for the specific group of weights. According to these results, identical weight values for PTAR and MP results in a best value at a time delay of −0.1 s. If the weight for PTAR is doubled while keeping the weight for MP the same, the result is still a best value at a time delay of −0.1 s. However, if the weight of MP is doubled while keeping the weight for PTAR at 1, the result is a best value at a time delay of 0 s.

TABLE 4.1 Best Case Index (*BCI*) for Different Weights and Wave Periods

Parameters			*BCI* for each wave period						
W1	*W2*	Time Delay (s)	5s	6s	7s	8s	9s	10s	11s
1	1	−0.2	2.02	1.47	1.30	1.26	1.24	1.29	1.28
1	1	−0.1	2.06	1.50	1.32	1.28	1.27	1.31	1.31
1	1	0	2.06	1.49	1.32	1.28	1.26	1.31	1.30
1	1	0.1	2.01	1.46	1.29	1.25	1.24	1.28	1.27
1	1	0.2	1.92	1.39	1.23	1.19	1.18	1.22	1.22
2	1	-0.2	3.05	2.20	1.96	1.91	1.89	1.95	1.93
2	1	-0.1	3.09	2.23	1.98	1.93	1.91	1.98	1.95
2	1	0	3.07	2.22	1.97	1.92	1.90	1.97	1.94
2	1	0.1	3.00	2.16	1.92	1.87	1.86	1.92	1.89
2	1	0.2	2.86	2.06	1.84	1.79	1.77	1.83	1.81
1	2	-0.2	3.02	2.20	1.94	1.86	1.84	1.91	1.91
1	2	-0.1	3.09	2.26	1.99	1.91	1.89	1.96	1.96
1	2	0	3.10	2.26	1.99	1.91	1.89	1.97	1.97
1	2	0.1	3.03	2.21	1.95	1.87	1.85	1.92	1.93
1	2	0.2	2.90	2.12	1.86	1.79	1.77	1.84	1.84

4.5 Study of Inertia and Friction in Complex WEC

In this study there were several sets of waves studied. As previously mentioned, the wave sets with 5s and 11s peak periods had to be added as cases to the code. These sets were not included in the original code and required some additional integral solving. As with the previous studies the output parameters were PTAR and MP. The range of inertia studied was 10, 15, 20 kg.m^2. The range of the friction parameter was 0, 0.005, 0.01, 0.015, 0.02. The friction had a unit of Nm.s/rad that is used very similar to damping in this model. In this study the optimal time delay was used, -0.1 seconds, to potentially reduce PTAR as the previous study in section 4.4 revealed. When calculating the peak to average ratio the last 40 percent of the simulation data was used. This was to ensure that the WEC was at steady state. Below is the data for the 8 second waves set both regular and irregular cases.

4.5.1 Regular Waves

With the regular waves a total simulation time was 120 seconds. The graph for wave set period 8 seconds is shown in Fig 4.7. From the graph it shows that as friction increases, the overall MP decreases. This makes sense as more energy is lost due to friction the less electricity is produced. It can also be observed that when the inertia increases the MP stays almost the exactly the same. In Fig. 4.8 the PTAR increased for friction values greater than 0.005. When more inertia was added the PTAR decreased but this additional amount was very minimal and it was less than 1% of the previous PTAR value. Also, it is important to note that when the friction is very low, the WEC control system was unstable. This study originally included an inertia value of 5 kg.m^2 ,but the data from those simulations was extremely erratic, on a scale of 100 times the other PTAR values, and thus wasn't included in the graphs.

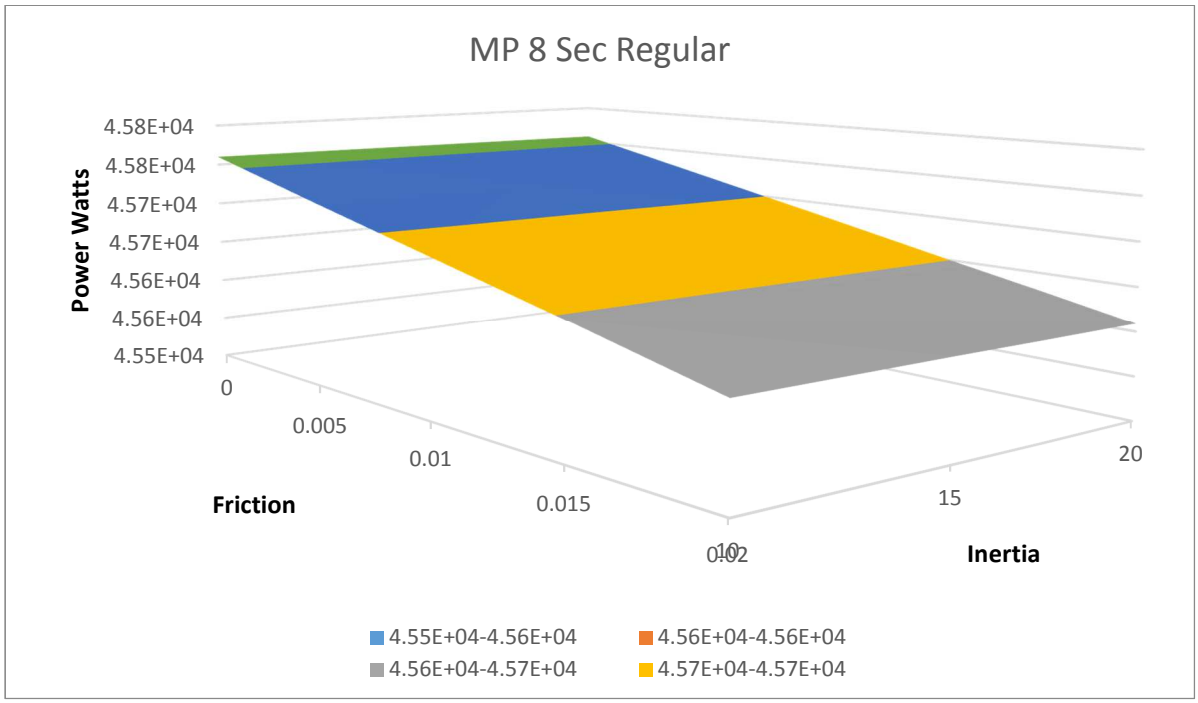

Fig. 4.7 Mean Power for 8 Second Period Regular Waves

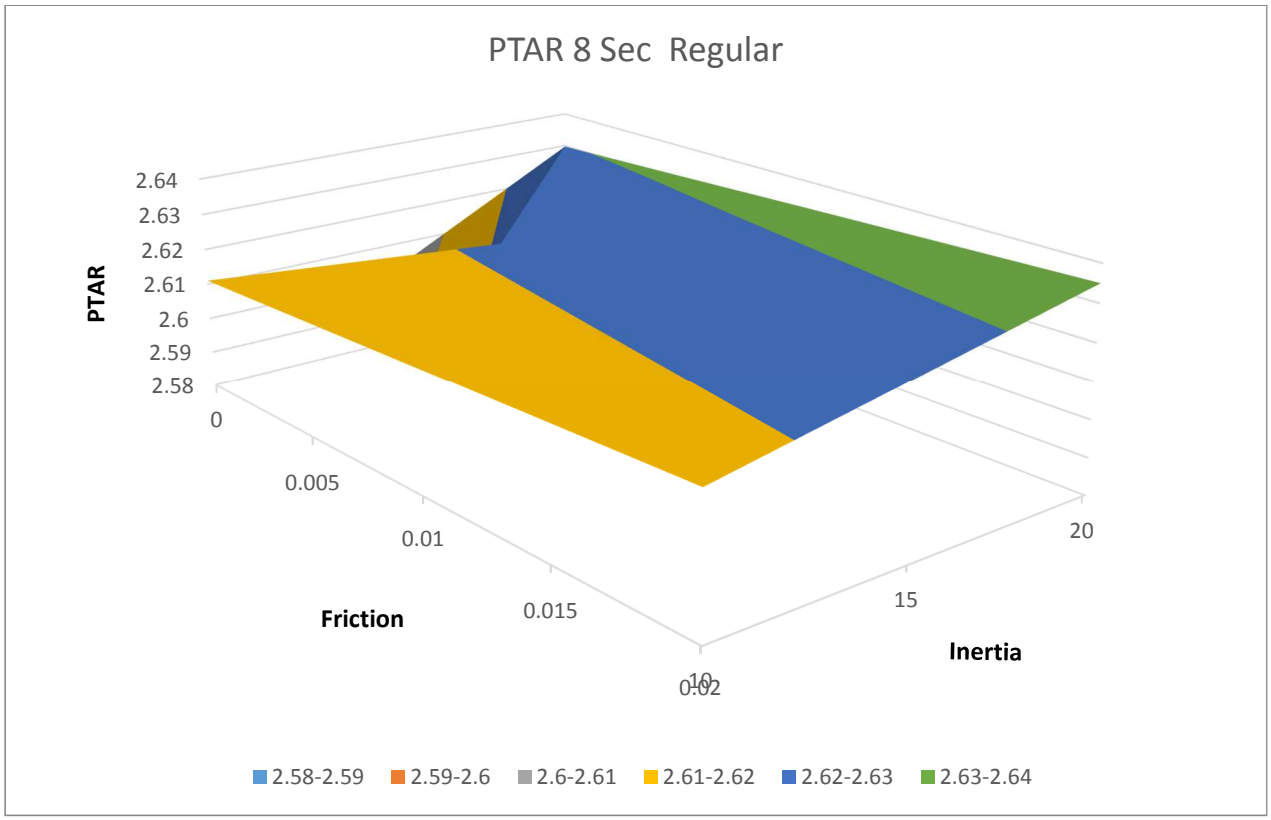

Fig. 4.8 Peak to Average Ratio 8 Second Regular Waves

4.5.2 Irregular Waves

When running the model in Simulink the time period of 500 seconds had to be used for the irregular waves. This particular WEC takes longer to yield approximately consistent results from one data set to another with irregular waves, which is the reason for the extended time. The PTAR and the MP can still be compared because PTAR and MP can be evaluated for any length of time. Once again irregular waves are more comparable to the real-world environment. In the MP graph of Fig 4.9 one can see that the general trend for friction is still the same. MP decreasing as the friction increases. With the inertia however, MP increased when more inertia was added. More power was produced over time when there was more inertia in the system. From the PTAR graph of Fig 4.10 it makes a much more interesting V-shape. With friction the PTAR follows the same trend as the 8 sec regular waves, as friction is increased the PTAR also increased. What is more interesting is that when the inertia is ran through its range, the inertia value of 15 kg.m^2 gives the lowest PTAR. This could be due to a few reasons, but the most likely

one is that this particular model, the complex with resonance control strategy, was initially optimized using that value for inertia. That way it would give the lowest PTAR with that inertia value and higher values of PTAR for any other inertia besides 15 kg.m^2.

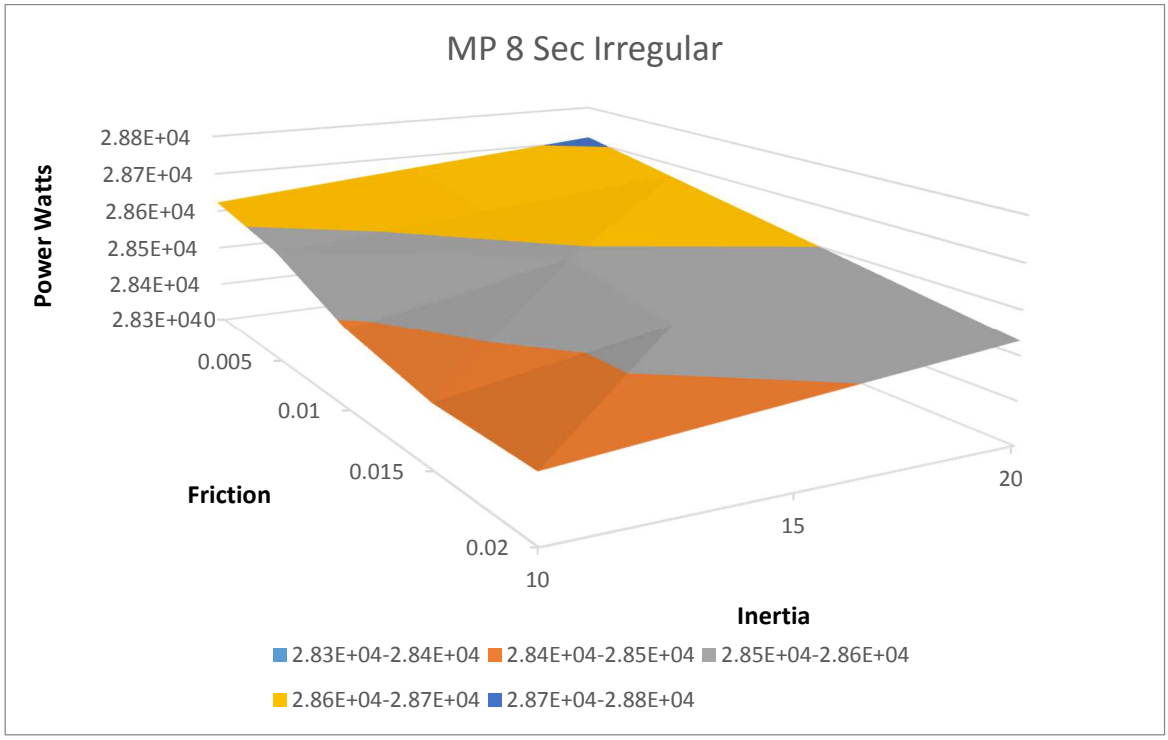

Fig. 4.9 Mean Power for 8 Second Period Irregular Waves

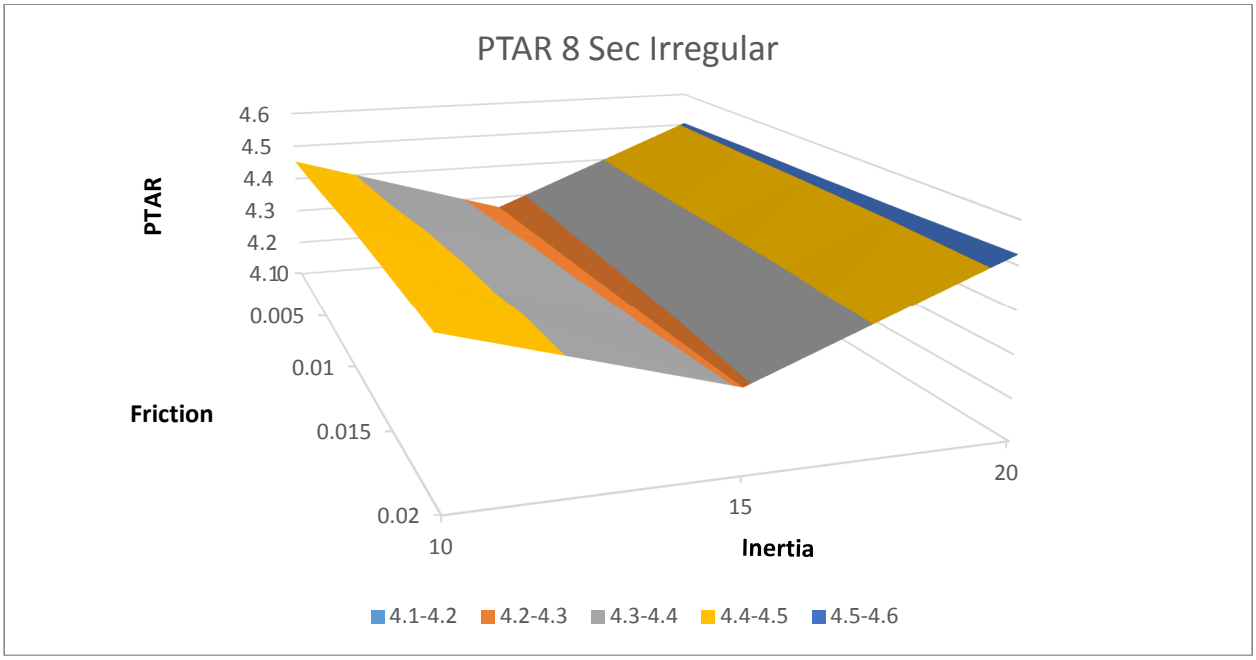

Fig. 4.10 Peak to Average Ratio for 8 Second Period Irregular Waves

One can also compare the two sets of graphs to each other. When directly comparing the MP regular to the MP irregular, one can observe that the regular wave produced much more power. This makes sense as irregular waves, if they are truly irregular, will sometimes counter act the motion of the buoy and thus less power is produced [12]. Also, the resonance control strategy takes basically no time at all, every half period, to make the generator sync up with the regular waves. When the control strategy is used with irregular waves it takes a few cycles before it synchronizes. Because these are irregular waves with the peak period being 8 seconds, but the control strategy is not aware of the peak period, so it is working very hard to keep the generator in resonance with the waves. These facts together give a reason that the MP is lower in the irregular waves. The MP extracted by the irregular waves is approximately 2/3 the power extracted by the regular waves. The PTAR is also significantly higher in irregular then regular due to similar reasons.

CHAPTER 5: CONCLUSION AND FUTURE WORK

There are multiple factors that influence the Peak to Average Ratio and the Mean Power in the wave energy conversion process. However, many of these factors are not independent of each other. As a result, a positive effect on the PTAR might cause a negative effect on the MP and vice versa. This conclusion can be drawn from the results discussed in Chapter 4. In the graph modifying bias and phase, there is a maximum mean power, i.e. the top of the dome shaped surface. This correlates to a PTAR that is not the lowest in the data set. One can reduce the PTAR, but at the expense of the MP. Since production of power is the main objective of a generator, it would be counterintuitive to do this.

5.1 Research Questions

To what extent can PTAR be reduced without sacrificing Mean Power?

Another significant observation from this thesis is the fact that the PTAR can not only be modified to any value by a phase difference between wave excitation force and buoy velocity, but it can also be reduced to an extent by it. An interesting observation is that the wave frequency is not noticed to affect where the peak power is produced. Highest mean power is always produced at a 0 sec time delay or 0° phase difference. A compromise between the MP and the PTAR is finally defined with a best-case index (*BCI*). It has been shown that similar weights given to the MP and the PTAR would result in a specific phase difference setting in the resonance control algorithm. The phase difference is only eliminated with the MP weight values being twice the PTAR weight values.

Is modification of inertia beneficial to the WEC by Reducing PTAR and maintaining MP?

With the last study one can easily conclude that there is a major difference in the effectiveness of this WEC when comparing regular and irregular waves. When comparing regular to irregular waves in this WEC model, PTAR is increased and MP is decreased in the irregular case. This is more indicative of a real-world situation where this WEC and control strategy is employed. There are indeed some trends that are independent of wave type. Increased friction decreases the MP and increases the PTAR regardless of wave type. The control strategy for the complex WEC model has the greatest effect on PTAR when the

inertia is set to be 15 kg.m^2. When the inertia is increased beyond 15 kg.m^2 the MP increases and so does the PTAR. When the inertia was changed it did have an effect on the MP and PTAR but both effects were minimal in a controlled WEC environment.

What parameters affect the PTAR and MP?

The phase delay had the largest impact in MP and PTAR. This was concluded in section 4.3. When the phase delay was +/- 50 degrees the PTAR was reduced substantially. The bias between the generator torque and PTO torque was an additional factor that reduced PTAR. However, this cannot be implemented with the complex resonance control WEC environment. The inertia also had an effect on the PTAR but it was less than 1% when increasing it by 5 kg.m^2.

5.2 Future Work

The observations and findings from the models investigated in this study call for a need for more complex models of the slider crank WEC. Future research efforts should try and utilize models that employ other methods and strategies, such as flywheels, to help regulate the PTAR and the MP of the WEC. Additionally, working with a hardware in the loop system can possible help answer some questions that arose from this thesis. Namely, a cost analysis that would allow one to determine an estimated cost reduction from using less versatile electrical components. A study involving the energy savings a flywheel energy storage system would also be informative.

REFERENCES

[1] https://www.zmescience.com/ecology/climate/how-much-renewable-energy/
"How Much Renewable Energy Does the World Use." ZME Science, 26 June 2018, www.zmescience.com/ecology/climate/how-much-renewable-energy/.

[2] M. Leijon et al, "Catch the wave to electricity," IEEE Power and Energy Magazine, vol. 7, (1), pp. 50-54, 2009
http://sedac.ciesin.columbia.edu/es/papers/Coastal_Zone_Pop_Method.pdf

[3] Kohari, Z., and I. Vajda. "Losses of flywheel energy storages and joint operation with solar cells." Journal of materials processing technology 161.1-2 (2005): 62-65.

[4]Diaz-González, F., Sumper, A., Gomis-Bellmunt, O. & Bianchi, F.D. 2013, "Energy management of flywheel-based energy storage device for wind power smoothing", Applied Energy, vol. 110, pp. 207-219.

[5] Y. Sang *et al*., "Resonance control strategy for a slider crank WEC power take-off system," in Proc. MTS/IEEE OCEANS '14, St. John's, Canada, 2014, pp. 1-8.

[6] Sjolte, Jonas, Gaute Tjensvoll, and Marta Molinas. "Power collection from wave energy farms." Applied Sciences 3.2 (2013): 420-436.

[7] Wang, Li, et al. "Study of a Hybrid Offshore Wind and Seashore Wave Farm Connected to a Large Power Grid through a Flywheel Energy Storage System." 2011 IEEE Power and Energy Society General Meeting, 2011, doi:10.1109/pes.2011.6039074.

[8] Khan, Md Rakib Hasan, et al. "Wave Excitation Force Prediction Methodology Based on Autoregressive Filters for Real Time Control." 2019 IEEE Green Technologies Conference (GreenTech). IEEE, 2019.

[9] Sjolte, Jonas, Gaute Tjensvoll, and Marta Molinas. "Power collection from wave energy farms." Applied Sciences 3.2 (2013): 420-436.

[10] Koker, Kristof L. De, et al. "Modeling of a Power Sharing Transmission in a Wave Energy Converter." 2016 IEEE 16th International Conference on Environment and Electrical Engineering (EEEIC), 2016, doi:10.1109/eeeic.2016.7555558.

[11]Sang, Yuanrui & Karayaka, H. & Yan, Yanjun & Zhang, James & Muljadi, Eduard & Yu, Yi-Hsiang. (2015). Energy extraction from a slider-crank wave energy converter under irregular wave conditions. 1-7. 10.23919/OCEANS.2015.7401873. 2015.

[12]Sang, Y., Karayaka, H. B., Yan, Y., Zhang, J. Z., Bogucki, D., & Yu, Y. H. (2017). A rule-based phase control methodology for a slider-crank wave energy converter power take-off system. International Journal of Marine Energy, 19, 124-144.

APPENDIX A: SOURCE CODE

%% Irregular Wave Force Generation "Irregular_Wave_Force.m"

```
clear;clc;close all;
%=========================================================================%
% initial inertia: 10
% initial viscous friction coefficient: 0.32

%=========================================================================%
%Callback for the simulink model
Ts=20e-6; % Sampling time
Td=1e-3; % Discrete Sampling time

%%% setting 1 %%%
gr=110;    % Gear ratio
%======================
aa=20e-6/(.5+20e-6);

%=========================================================================%
%Slider-Crank initialization
global r                    % Radius of crank. used again in the rk4sys_step
function and slider crank function.
global l                    % Length of rod, used again in the slider crank
function.
global dr_dsb                    % (Used to be r+A) Distance between the
lowest edge of the crank and the reference water surface
r=.5;                     % Radius of crank. used again in the rk4sys_step
function and slider crank function.
l=1;                       % Length of rod, used again in the slider crank
function.
lambda=r/l;                % used again in the slider crank function.
B=0.01;                   % Viscous friction, used again in the slider crank
function.
J=10;                    % inertia of flywheel, used again in the slider crank
function.
dr_dsb=l;                    % (Used to be r+A) Distance between the lowest
edge of the crank and the reference water surface
mcrp=10;                % Total of mass of piston (or slider) and connecting
rod respectively.

%=========================================================================%
% Hydrodynamics initialization (frequency domain)
delta_omega=0.01;
omega=0.5:delta_omega:1.4;
N=length(omega);
fn=omega/2/pi;% frequencies of the wave components
%%%=======================================%%%
%%% Settings for irregular wave parameters %%%
% Equivalent energy transfer: Hm0=2*sqrt(2)*A  (A is the amplitude of the
regular wave)
```

```
Hm0=sqrt(2); % significant wave height of the irregular wave. The same value
is used as that in "Effect of..."
Tp=6; % If this changes, int_S_star has to be recalculated. Peak period of
the irregular wave. In "Effect of...", they used an average period of 6. We
can use our own to make the spectrum fit our need.
%%%=========================================%%%
fp=1/Tp;
g=9.81; % gravity acceleration
rho=1020;% water density

%=========================================================================%
% Choose Spectrum for the System:
flag = 1; % 0 for Breschneider model and 1 for JONSWAP Model

switch flag
    case 0
% ====================  Bretschneider model  ============================%
%         R=(Tp/1.057)^(-4); % These are calculated separately for the sake
of the organing the formula
%         Q=R*Hm0^2/4;% These are calculated separately for the sake of the
organing the formula
%         S=Q*fn.^(-5).*exp(-R*fn.^(-4)); % Bretschneider spectrum ("sea
spectra revisited" or MIT OCW slides)
        S=Hm0^2/4*(1.057*fp)^4*fn.^(-5).*exp(-5/4*(fp./fn).^4); %According to
WEC_Sim_User_Manual_v1.0.pdf
    case 1
% ====================  JONSWAP Model ==================================%
        m0=sqrt(Hm0/4); % wave field variance. See "On control ...".
        %alpha=0.0081; % a given constant which is used in most references,
see "sea spectra revisited".
        gamma=6;% If this changes, int_S_star has to be recalculated. The
average of gamma is 3.3 (see "sea spectra revisited"). enhancement factor by
which the P_M peak energy is multiplied to get the peak energy value of the
spectrum.
        %Increasing gamma has the effect of reducing the spectral bandwidth,
        %thereby increasing periodicity of the wave field. See "On control
...".
        for i2=1:N
            if fn(i2)<=fp
                sigma=0.07;%if f<fp  sigma is the width factor of the
enhanced peak, see "sea spectra revisited". The numbers are given in "sea
spectra revisited".
            elseif fn(i2)>fp
                sigma=0.09;%if f>fp
            end

%=========================================================================%
            % the following eqn is from On Control of a Pitching and Surging
Wave Energy Converter-HYavuz.pdf
            %     S(i2)=5*m0/fp*((fp/fn(i2))^5)*exp(-
5/4*((fp/fn(i2))^4))*gamma^exp(-(fn(i2)/fp-1/(2*sigma^2)));

%=========================================================================%
            % the following eqn is from sea_spectra_revisited.pdf and
Measurements of wind-wave growth and swell decay during the Joint North Sea
Wave Project (JONSWAP)_Jonswap-Hasselmann1973.pdf
```

```
            %     S(i2)=alpha*g^2*(2*pi)^(-4)*fn(i2)^(-5)*exp(-
5/4*((fp/fn(i2))^4))*gamma^exp(-(fn(i2)-fp)^2/(2*sigma^2*fp^2));

%=========================================================================%
            % The following eqn uses basic spectrum from "On control ..." and
peak enhancement factor from "Sea_spectra_revisited".
            S(i2)=5*m0/fp*((fp/fn(i2))^5)*exp(-
5/4*((fp/fn(i2))^4))*gamma^exp(-(fn(i2)-fp)^2/(2*sigma^2*fp^2));

%=========================================================================%
            % The following eqn is according to WEC_Sim_User_Manual_v1.0.pdf
            % integral of
            % 9.81^2/(2*pi)^4*x^(-5)*exp(-5/4*(0.125/x)^4)*6^exp(-((x/0.125-
1)/(sqrt(2)*0.07))^2)
            % from 0 to 0.125 = 37.61 calculated by Wolframalpha
            % integral of
            % 9.81^2/(2*pi)^4*x^(-5)*exp(-5/4*(0.125/x)^4)*6^exp(-((x/0.125-
1)/(sqrt(2)*0.09))^2)
            % from 0.125 to infinity=65.8056 calculated by Wolframalpha
            switch Tp
                case 5
                    int_S_star=5.7388+10.0411;
                case 6
                    int_S_star=11.9001+20.8213;
                case 7
                    int_S_star=22.0463+38.574;
                case 8
                    int_S_star=37.61+65.8056;
                case 9
                    int_S_star=60.244+105.408;
                case 10
                    int_S_star=91.8214+160.658;
                case 11
                    int_S_star=134.436+235.22
            end
            alpha=Hm0^2/(int_S_star*16); %int_S_star should be changed when
Tp or gamma changes.
            GAMMA=exp(-((fn(i2)/fp-1)/(sqrt(2)*sigma))^2);
            S(i2)=alpha*g^2/(2*pi)^4*fn(i2)^(-5)*exp(-
5/4*(fp/fn(i2))^4)*gamma^GAMMA;
        end
end
 plot(omega/(2*pi),S)
 grid on
 axis([0.08 0.26 0 3.5])
 xlabel('f (Hz)')
 ylabel('Spectral Density (m^2s)')
 title('JONSWAP Spectrum')

%=========================================================================%
% Wave elevation and excitation force (time domain)
Start_Time=0;              % time start
End_Time=500;              % final time
Interval=0.01;             % sampling time interval
t=Start_Time:Interval:End_Time;
M=length(t);
```

```
%%% setting 2 %%%
a=5; % buoy radius
%======================
c=rho*g*pi*a^2; % a coefficient that is used later
%%% setting 3 %%%
A=sqrt(2*S*delta_omega/2/pi); % calculate amplitude for each wave component
%======================
%%% setting 5 %%%
Phase=2*pi*rand(1,N); % randomly generate the initial phase of each wave
component
%======================

Ka=[0 0.05 0.1 0.2 0.3 0.4 0.5 0.6 0.7 0.8 0.9 1.0 1.2 1.4 1.6 1.8 2.0 2.5
3.0 4.0 5.0 6.0 7.0 8.0 9.0 10.0]';
Amass=[0.8310 0.8764 0.8627 0.7938 0.7157 0.6452 0.5861 0.5381 0.4999 0.4698
0.4464 0.4284 0.4047 0.3924 0.3871 0.3864 0.3884 0.3988 0.4111 0.4322 0.4471
0.4574 0.4647 0.4700 0.4740 0.4771]';
Damping=[0 0.1036 0.1816 0.2793 0.3254 0.3410 0.3391 0.3271 0.3098 0.2899
0.2691 0.2484 0.2096 0.1756 0.1469 0.1229 0.1031 0.0674 0.0452 0.0219 0.0116
0.0066 0.0040 0.0026 0.0017 0.0012]';
len=length(Ka);
kappa=zeros(1,len);
imkap=zeros(1,len);
rekap=zeros(1,len);
mm=rho*(2*pi/3)*a^3;
Sb=rho*g*pi*a^2;%785890;
kappa(1)=1;
imkap(1)= 2*Damping(1)*Ka(1)/3;
rekap(1)= sqrt(kappa(1)^2-imkap(1)^2);
for j=2:len
    kappa(j)= sqrt(4*Damping(j)/(3*pi*Ka(j)));
    imkap(j)= 2*Damping(j)*Ka(j)/3;
    rekap(j)= sqrt(kappa(j)^2-imkap(j)^2);
end

Kaq=omega.^2/g*a;
kappa_im=zeros(1,N);
kappa_re=zeros(1,N);
kappa_angle=zeros(1,N);
kappa_abs=zeros(1,N);
for i1=1:N
    kappa_abs(i1)=interp1(Ka,kappa,Kaq(i1),'cubic');
    kappa_im(i1)=interp1(Ka,imkap,Kaq(i1),'cubic');
    kappa_re(i1)=interp1(Ka,rekap,Kaq(i1),'cubic');
    kappa_angle(i1)=atan(kappa_im(i1)/kappa_re(i1));
end
%%%
% kap=0.502764572022028;
%%%
% eta=zeros(1,M);
% Fe=zeros(1,M); % initialization for wave force at each time point
Fe=@(t)0;
eta_total=@(t)0;
%%% setting 5 %%%
% omega=2*pi/6*ones(1,N);
```

```
% kappa_angle=0;
%======================
for i=1:N
    eta{i}=@(t)A(i)*sin(omega(i)*t+Phase(i)+kappa_angle(i));
    Fe_components{i}=@(t)c*kappa_abs(i)*eta{i}(t);
    Fe=@(t)Fe(t)+Fe_components{i}(t);
    eta_total=@(t)eta_total(t)+eta{i}(t);
end
%
Fe=@(t)kap*rho*g*pi*a^2*(eta{1}(t)+eta{2}(t)+eta{3}(t)+eta{4}(t)+eta{5}(t)+et
a{6}(t)+eta{7}(t)+eta{8}(t)+eta{9}(t)+eta{10}(t));%zw(t);

% for i=1:M
%     eta(i)=sum(A.*sin(omega*t(i)+Phase));
%     Fe(i)=sum(c*kappa_abs.*A.*sin(omega*t(i)+Phase+kappa_angle));
% end
figure;
% subplot(2,1,1)
% plot(t,eta);
% grid
% title('wave elevation')

% subplot(2,1,2)
plot(t,Fe(t));
grid
%title('excitation force')
xlabel('Time(s)')
ylabel('Excitation Force')
% hold on;
figure;
plot(t,eta_total(t));
grid
title('wave elevation')
Ocean_Wave_AccP.signals.values=Fe(t)';
Ocean_Wave_AccP.time=t';
```

%% Regular Wave Force Generation “mechanical_energy.m”

```
% clear;clc;close all;
%=========================================================================%
% initial inertia: 10
% initial viscous friction coefficient: 0.32

%=========================================================================%
%Callback for the simulink model
Ts=20e-6; % Sampling time
T_d=1e-3; % Discrete Sampling time

%%% setting 1 %%%
gr=110;    % Gear ratio
%======================
aa=20e-6/(.5+20e-6);

%=========================================================================%
%==========================Initialization=================================%

% global Interval A r l lambda B J L_af V_f r_f I_f L_aa r_a kv dr m R Sb

% %Hydrodynamics initialization
% Start_Time=0;             % time start
% End_Time=500;              % final time
% Interval=0.01;            % simpling time interval
rho=1020;                 % the density of water
g=9.81;                   % acceleration of gravity
a=5;%0.9533;                % buoy radius
% Rv=10;                  % Viscous force coefficient
% Rf=0;                     % Friction force coefficient
%
% %omega=1;                  % The angular velocity of water wave
% A=0.5;                    % The maximum amplitude of water wave,
initialized again in the slider crank function.
% f=1/10;                     % The frequency of water wave
% omega=2*pi*f;             % The angular velocity of water wave
% k=omega^2/g;              % Wave number for infinite water depth
% Kaq=k*a;                  % ka
%
% zw=@(t)A*sin(omega*t+288*pi/180);    % the function of water wave

%Slider-Crank initialization
global r                    % Radius of crank. used again in the rk4sys_step
function and slider crank function.
global l                    % Length of rod, used again in the slider crank
function.
global dr_dsb                   % (Used to be r+A) Distance between the
lowest edge of the crank and the reference water surface
r=0.5;                    % Radius of crank. used again in the rk4sys_step
function and slider crank function.
l=1;                      % Length of rod, used again in the slider crank
function.
lambda=r/l;               % used again in the slider crank function.
```

```
B=0.01;                   % Viscous friction, used again in the slider crank
function.
J=10;                    % inertia of flywheel, used again in the slider crank
function.
dr_dsb=l;                 % sqrt(l^2-r^2);                 % Distance between
the lowest edge of the crank and the reference water surface
mcrp=10;                 % Total of mass of piston (or slider) and connecting
rod respectively.

%Fu=zeros(1,(End_Time-Start_Time)/Interval+1);

% %Generator initialization
% L_af = 1.234; % Mutual inductance between the field and the rotating
armature coils.
% V_f = 220; % Field voltage.
% r_f = 150; % Resistance of field windings
% I_f = V_f/r_f; % Current of field windings
% L_aa = 0.016; % Self-inductance of the field and armature windings.
% r_a = 0.78;  % Resistance of the armature coils.
% kv = L_af*I_f; % Stator constant

%=========================================================================%
% %===Calculating mu, epsilon and kappa through graphical observation======%
%
% Ka=[0 0.05 0.1 0.2 0.3 0.4 0.5 0.6 0.7 0.8 0.9 1.0 1.2 1.4 1.6 1.8 2.0 2.5
3.0 4.0 5.0 6.0 7.0 8.0 9.0 10.0]';
% Amass=[0.8310 0.8764 0.8627 0.7938 0.7157 0.6452 0.5861 0.5381 0.4999
0.4698 0.4464 0.4284 0.4047 0.3924 0.3871 0.3864 0.3884 0.3988 0.4111 0.4322
0.4471 0.4574 0.4647 0.4700 0.4740 0.4771]';
% Damping=[0 0.1036 0.1816 0.2793 0.3254 0.3410 0.3391 0.3271 0.3098 0.2899
0.2691 0.2484 0.2096 0.1756 0.1469 0.1229 0.1031 0.0674 0.0452 0.0219 0.0116
0.0066 0.0040 0.0026 0.0017 0.0012]';
%
% kappa(1)=1;
% for i=2:length(Ka)
%     kappa(i)=sqrt(4*Damping(i)/(3*pi*Ka(i)));
% end
%
% Mu = interp1(Ka,Amass,Kaq','cubic');
% Ep = interp1(Ka,Damping,Kaq','cubic');
% kap= interp1(Ka,kappa,Kaq','cubic');

%=========================================================================%
%Calculating Coefficients of the Differential Equation of Buoy Displacement
dr_dsb=1;
Sb=rho*g*pi*a^2;%785890;
mm=rho*(2*pi/3)*a^3;
% m=mm*(1+Mu);%267040+156940;
% R=Rv+Rf+Ep*omega*mm;%91520;
% Fe=@(t)kap*rho*g*pi*a^2*zw(t);
% t = Start_Time:Interval:End_Time;

% figure;
% % subplot(2,1,1)
% % plot(t,eta);
% % grid
```

```
% % title('wave elevation')
%
% % subplot(2,1,2)
% plot(t,Fe(t));
% grid
% title('excitation force')
% % hold on;
% figure;
% plot(t,zw(t));
% grid
% title('wave elevation')
% Ocean_Wave_AccP.signals.values=Fe(t)';
% Ocean_Wave_AccP.time=t';

%Call to find initial angle
Theta_Initial=Initial_Angle_Solver();
[bs,as]=RadiationKomega(a,T_d);
% load az
% load bz
Wave_Analysis;

%Calculate initial position in case of complex conjugate control
% init_z=-max((Fe(t)/(4*R*pi*f)))
```

```
%% Peak to average Ratio script %%


format short
format compact
starti=round(0.4*length(Power.time)); % Last 40% of data
Average_Power=max(Energy)/End_time    %Evaluated for end time
Max_p = max(Power.Data(start:end))
Mean_p = mean(Power.Data(starti:end))
PTARC = Max_p/Mean_p              % Named PTARC b/c matlab naming convention
```

%% Initial angel solver function “Initial_Angle_Solver.m”

```
function Theta_Initial=Initial_Angle_Solver()
format long;
%=========================================================================%
%Slider-Crank initialization

global r                    % Radius of crank. used again in the rk4sys_step
function and slider crank function.
global l                    % Length of rod, used again in the slider crank
function.
global dr_dsb                   % (Used to be r+A) Distance between the
lowest edge of the crank and the reference water surface
%=========================================================================%

f1=@(u)(dr_dsb-sqrt(l^2-(r*sin(u))^2))/r;
f2=@(u)cos(u);
Theta_Initial=pi/2;
err=1;
while err>1e-12
    f1n=f1(Theta_Initial);
    f2n=f2(Theta_Initial);
    Theta_Initial=acos(f1n);
    err=abs(f1n-f2n);
end
disp('The Initial Angle is (in radian): ');
disp(Theta_Initial);
disp('In degrees: ');
disp(Theta_Initial/pi*180);
```

APPENDIX B: DATA TABLES

Data from Study 4. Regular and Irregular waves. The sets with the inertia being 5 were not used in the above graphs and as one can see from the tables below those data entries are quite erratic.

Regular Waves

Regular										
Wave (Period)		J		B		Time (120s)		MP		PTAR
	5		5		0			1.0395E+07		506.82
	5		5		0.005			1.16E+07		903.88
	5		5		0.01			1.0704E+07		499.35
	5		5		0.015			1.16E+07		1547
	5		5		0.02			1.15E+07		452
	5		10		0			2.82E+04		3.977
	5		10		0.005			2.82E+04		3.9877
	5		10		0.01			2.81E+04		3.9979
	5		10		0.015			2.80E+04		4.008
	5		10		0.02			2.79E+04		4.0183
	5		15		0			2.82E+04		3.999
	5		15		0.005			2.82E+04		4.0092
	5		15		0.01			2.81E+04		4.0194
	5		15		0.015			2.80E+04		4.0297
	5		15		0.02			2.79E+04		4.04
	5		20		0			2.82E+04		4.0183
	5		20		0.005			2.82E+04		4.0285
	5		20		0.01			2.81E+04		4.0388
	5		20		0.015			2.80E+04		4.0491
	5		20		0.02			2.79E+04		4.0595
Wave (Period)		J		B				MP		PTAR
	6		5		0			1.16E+07		961.91
	6		5		0.005			1.15E+07		446.51
	6		5		0.01			1.14E+07		1.93E+03
	6		5		0.015			1.17E+07		1.55E+03
	6		5		0.02			1.14E+07		431.7
	6		10		0			3.82E+04		2.7991
	6		10		0.005			3.82E+04		2.8022
	6		10		0.01			3.81E+04		2.8053
	6		10		0.015			3.80E+04		2.8084
	6		10		0.02			3.80E+04		2.8116
	6		15		0			3.82E+04		2.108
	6		15		0.005			3.82E+04		2.8139

Wave (Period)	J	B		MP	PTAR	
7	5	0		11782000	443.78	
7	5	0.005		11818000	633.23	
7	5	0.01		11581000	2512	
7	5	0.015		11706000	538.46	
7	5	0.02		11689000	353.58	
7	10	0		43217	2.6754	
7	10	0.005		43168	2.677	
7	10	0.01		43180	2.679	
7	10	0.015		43071	2.681	
7	10	0.02		43022	2.6829	
7	15	0		43240	2.6862	
7	15	0.005		43156	2.6881	
7	15	0.01		43107	2.69	
7	15	0.015		43058	2.6919	
7	15	0.02		43009	2.6937	
7	20	0		43192	2.6973	
7	20	0.005		43143	2.6992	
7	20	0.01		43094	2.7011	
7	20	0.015		43045	2.703	
7	20	0.02		42997	2.7049	
Wave (Period)	J	B		MP	PTAR	
8	5	0		11756000	426	
8	5	0.005		11809000	1243.1	
8	5	0.01		11614000	389.46	
8	5	0.015		11757000	506	
8	5	0.02		11692000	1636.9	
8	10	0		45760	2.611	
8	10	0.005		45722	2.6123	
8	10	0.01		45685	2.6136	
8	10	0.015		45648	2.6149	
8	10	0.02		45610	2.6162	
8	15	0		45759	2.603	
8	15	0.005		45722	2.6216	
8	15	0.01		45684	2.6229	
8	15	0.015		45647	2.6242	
8	15	0.02		45610	2.6255	
8	20	0		45758	2.6297	
8	20	0.005		45721	2.631	
8	20	0.01		45684	2.6324	

Wave (Period)	J	B		MP	PTAR	
9	5	0		11614000	570.95	
9	5	0.005		11401000	1694.7	
9	5	0.01		11487000	2021.1	
9	5	0.015		11735000	540.6	
9	5	0.02		11700000	1070.9	
9	10	0		45835	2.5947	
9	10	0.005		45805	2.5957	
9	10	0.01		45776	2.5967	
9	10	0.015		45746	2.5977	
9	10	0.02		45717	2.5987	
9	15	0		45836	2.6034	
9	15	0.005		45807	2.6044	
9	15	0.01		45777	2.6055	
9	15	0.015		45748	2.6065	
9	15	0.02		45718	2.6075	
9	20	0		45838	2.6121	
9	20	0.005		45808	2.6131	
9	20	0.01		45779	2.6142	
9	20	0.015		45749	2.6152	
9	20	0.02		45720	2.6162	
Wave (Period)	J	B		MP	PTAR	
10	5	0		11411700	1823.8	
10	5	0.005		11519000	9094.9	
10	5	0.01		11519000	9094.9	
10	5	0.015		1.1702	404.36	
10	5	0.02		11749000	376.28	
10	10	0		43816	2.6638	
10	10	0.005		43792	2.6647	
10	10	0.01		43768	2.6656	
10	10	0.015		43744	2.6665	
10	10	0.02		43720	2.6674	
10	15	0		43813	2.6724	
10	15	0.005		43789	2.6733	
10	15	0.01		43765	2.6742	
10	15	0.015		43741	2.6751	
10	15	0.02		43717	2.676	
10	20	0		43810	2.6811	

Wave (Period)	J	B		MP	PTAR	
11	5	0		11763000	377.91	
11	5	0.005		11704000	1946.1	
11	5	0.01		11685000	1893.5	
11	5	0.015		11724000	440.4	
11	5	0.02		11803000	456.76	
11	10	0		43109	2.6136	
11	10	0.005		43089	2.6144	
11	10	0.01		43070	2.6151	
11	10	0.015		43050	2.6158	
11	10	0.02		43030	2.6165	
11	15	0		43108	2.6177	
11	15	0.005		43088	2.619	
11	15	0.01		43069	2.6203	
11	15	0.015		43049	2.6215	
11	15	0.02		43029	2.6225	
11	20	0		43107	2.6198	
11	20	0.005		43088	2.6211	
11	20	0.01		43068	2.6224	
11	20	0.015		43048	2.6236	
11	20	0.02		43028	2.6247	

Irregular Wave Data

Irregular						
Wave (Period)	J	B	Time (500	MP	PTAR	
5	10	0		4854	31.9263	
5	10	0.005		4761.7	32.5374	
5	10	0.01		4670.7	33.1643	
5	10	0.015		4578	33.83	
5	10	0.02		4487	34.5091	
5	15	0		4912.6	31.6107	
5	15	0.005		4822.3	32.1948	
5	15	0.01		4730.3	32.8159	
5	15	0.015		4638	33.4658	
5	15	0.02		4547.4	34.1251	
5	20	0		4964.1	31.3407	
5	20	0.005		4872.1	31.925	
5	20	0.01		4781.4	32.5263	
5	20	0.015		4689.6	33.1564	
5	20	0.02		4598.6	33.8053	
Wave (Period)	J	B	Time (500	MP	PTAR	
6	10	0		20881	7.3002	
6	10	0.005		20812	7.3231	
6	10	0.01		20742	7.3461	
6	10	0.015		20673	7.3693	
6	10	0.02		20604	7.3927	
6	15	0		20931	7.2059	
6	15	0.005		20862	7.2286	
6	15	0.01		20793	7.2516	
6	15	0.015		20724	7.207	
6	15	0.02		20650	7.297	
6	20	0		20983	7.138	
6	20	0.005		20914	7.1607	
6	20	0.01		20844	7.1835	
6	20	0.015		20962	7.1448	
6	20	0.02				
Wave (Period)	J	B	Time (500	MP	PTAR	

7	10	0		2.28E+04	7.201	
7	10	0.005		2.27E+04	7.2148	
7	10	0.01		2.27E+04	7.2296	
7	10	0.015		2.26E+04	7.2446	
7	10	0.02		2.26E+04	7.2595	
7	15	0		2.29E+04	6.8694	
7	15	0.005		2.28E+04	6.8836	
7	15	0.01		2.28E+04	6.8978	
7	15	0.015		2.27E+04	6.9122	
7	15	0.02		2.27E+04	6.9267	
7	20	0		2.30E+04	6.635	
7	20	0.005		2.29E+04	6.6488	
7	20	0.01		2.29E+04	6.6626	
7	20	0.015		2.28E+04	6.6766	
7	20	0.02		2.28E+04	6.6906	
Wave (Period)	J	B	Time (500	MP	PTAR	
8	10	0		2.86E+04	4.4533	
8	10	0.005		2.86E+04	4.4595	
8	10	0.01		2.85E+04	4.4707	
8	10	0.015		2.84E+04	4.4726	
8	10	0.02		2.84E+04	4.4726	
8	15	0		2.87E+04	4.267	
8	15	0.005		2.86E+04	4.2734	
8	15	0.01		2.86E+04	4.2786	
8	15	0.015		2.85E+04	4.2848	
8	15	0.02		2.85E+04	4.2937	
8	20	0		2.87E+04	4.5054	
8	20	0.005		2.87E+04	4.51	
8	20	0.01		2.86E+04	4.5125	
8	20	0.015		2.86E+04	4.5168	
8	20	0.02		2.85E+04	4.5242	

9	10	0		31335	4.9591	
9	10	0.005		31309	4.9898	
9	10	0.01		31283	4.9911	
9	10	0.015		31257	4.9917	
9	10	0.02		31231	4.9837	
9	15	0		32084	4.4878	
9	15	0.005		32057	4.4917	
9	15	0.01		32030	4.4965	
9	15	0.015		32004	4.4994	
9	15	0.02		31977	4.5033	
9	20	0		32723	4.3043	
9	20	0.005		32696	4.308	
9	20	0.01		32668	4.3117	
9	20	0.015		32641	4.3154	
9	20	0.02		32614	4.319	
Wave (Period)	J	B	Time (500	MP	PTAR	
10	10	0		28500	4.6805	
10	10	0.005		28478	4.6542	
10	10	0.01		28455	4.6873	
10	10	0.015		28432	4.6902	
10	10	0.02		28409	4.6962	
10	15	0		29219	4.4071	
10	15	0.005		29196	4.4115	
10	15	0.01		29173	4.4091	
10	15	0.015		29150	4.415	
10	15	0.02		29126	4.4153	
10	20	0		29725	4.2072	
10	20	0.005		29702	4.2083	
10	20	0.01		29678	4.2128	
10	20	0.015		29655	4.2146	
10	20	0.02		29631	4.216	

Wave (Period)	J	B	Time (500	MP	PTAR	
11	10	0		15187	18.9829	
11	10	0.005		15179	18.9088	
11	10	0.01		15163	18.9085	
11	10	0.015		15148	18.8544	
11	10	0.02		15133	18.9049	
11	15	0		19940	14.8057	
11	15	0.005		19921	14.8029	
11	15	0.01		19909	15.1674	
11	15	0.015		20039	14.4873	
11	15	0.02		20027	14.6671	
11	20	0		176520	13.1063	
11	20	0.005		17633	13.1151	
11	20	0.01		17609	13.105	
11	20	0.015		17590	13.0989	
11	20	0.02		1756800	13.0822	

Data from Excel Polyfit for Waves 5,6,7,8,9,10,11

	(1/11)		(1/10)		(1/9)		(1/8)	
55	4.78255		4.638222		5.153929		5.485891	
52.5	4.498268		4.39231		4.86017		5.17266	
50	4.2596		4.1846		4.61115		4.90325	
47.5	4.058375		4.008527		4.398637		4.669721	
45	3.887613		3.858428		4.215616		4.465329	
42.5	3.741412		3.729459		4.056172		4.284412	
40	3.61484		3.61752		3.91538		4.12228	
37.5	3.503832		3.519181		3.789204		3.975112	
35	3.405093		3.431612		3.674395		3.839857	
32.5	3.316005		3.35252		3.568399		3.714139	
30	3.23454		3.28008		3.46927		3.59617	
27.5	3.15918		3.212883		3.375584		3.484668	
25	3.088838		3.149873		3.286365		3.378777	
22.5	3.022788		3.090304		3.201009		3.277999	
20	2.9606		3.03368		3.11922		3.18212	
17.5	2.902076		2.97972		3.040947		3.091155	
15	2.8472		2.928312		2.966326		3.005289	
12.5	2.796083		2.879474		2.895632		2.924822	
10	2.74892		2.83332		2.82923		2.85013	
7.5	2.705952		2.790032		2.767535		2.781619	
5	2.667428		2.749828		2.710979		2.719691	
2.5	2.633581		2.712942		2.659975		2.664715	
0	2.6046		2.6796		2.6149		2.617	
-2.5	2.580612		2.650005		2.576069		2.576777	
-5	2.561673		2.624322		2.543722		2.544185	
-7.5	2.547753		2.602672		2.518019		2.519259	
-10	2.53874		2.58512		2.49903		2.50193	
-12.5	2.53444		2.571676		2.486741		2.492024	
-15	2.534583		2.562293		2.481057		2.48927	
-17.5	2.538841		2.556875		2.48182		2.49331	
-20	2.54684		2.55528		2.48882		2.50372	
-22.5	2.55819		2.557333		2.50182		2.520028	
-25	2.57251		2.562842		2.520584		2.541746	
-27.5	2.589464		2.571615		2.54491		2.5684	
-30	2.6088		2.58348		2.57467		2.59957	
-32.5	2.630394		2.598314		2.60985		2.634933	
-35	2.654303		2.616068		2.650601		2.674314	
-37.5	2.680817		2.636803		2.697295		2.717735	
-40	2.71052		2.66072		2.75058		2.76548	
-42.5	2.744359		2.688206		2.81145		2.818158	
-45	2.783713		2.719872		2.88131		2.876772	
-47.5	2.830467		2.756602		2.962055		2.942795	
-50	2.8871		2.7996		3.05615		3.01825	
	$R^2 = 0.9997$		$R^2 = 0.9993$		$R^2 = 0.9997$		$R^2 = 0.9999$	

	(1/7)		(1/6)		(1/5)	
	5.96977		8.794964		5.12192	
	5.554537		8.077016		5.482938	
	5.2247		7.3965		5.76995	
	4.959843		6.762929		5.986186	
	4.74307		6.182908		6.135838	
	4.560636		5.660487		6.22389	
	4.4016		5.1975		6.25596	
	4.257494		4.79388		6.238149	
	4.122008		4.447964		6.176894	
	3.990697		4.156778		6.07884	
	3.8607		3.9163		5.95071	
	3.73048		3.721713		5.799192	
	3.599583		3.567633		5.630829	
	3.468407		3.448325		5.451922	
	3.338		3.3579		5.26844	
	3.209867		3.29049		5.085937	
	3.085795		3.240414		4.909483	
	2.967704		3.202317		4.743595	
	2.8575		3.1713		4.59219	
	2.756964		3.143025		4.458531	
	2.667645		3.113808		4.345195	
	2.590774		3.080691		4.254043	
	2.5272		3.0415		4.1862	
	2.477337		2.994879		4.142044	
	2.441133		2.940314		4.121206	
	2.418057		2.878135		4.122574	
	2.4071		2.8095		4.14431	
	2.406795		2.736365		4.183874	
	2.415258		2.661433		4.238056	
	2.430239		2.588085		4.303023	
	2.4492		2.5203		4.37436	
	2.469403		2.462546		4.44714	
	2.48802		2.419664		4.515985	
	2.502257		2.396731		4.575147	
	2.5095		2.3989		4.61859	
	2.507473		2.431233		4.64009	
	2.49442		2.498508		4.633333	
	2.4693		2.605008		4.59203	
	2.432		2.7543		4.51004	
	2.383567		2.948991		4.381494	
	2.326458		3.190464		4.200939	
	2.264805		3.478604		3.963482	
	2.2047		3.8115		3.66495	

APPENDIX C: SC-WEC RESONANCE CONTROL ALGORITHM WITHOUT OVERLAY